Remote Sensing of Ocean Color

2 authors, including:

Heidi M Dierssen
University of Connecticut
102 PUBLICATIONS   **2,754** CITATIONS

Some of the authors of this publication are also working on these related projects:

Hyperspectral Infrared Imager (HyspIRI) - Aquatic Study Group (ASG) View project

Remote Sensing of Ocean Color

Glossary Absorption, a(λ) The fraction of a collimated beam of photons in a particular wavelength (λ), which is absorbed or scattered per unit distance within the medium (units 1/length or m^{-1}). Photons which are absorbed by ocean water alter the spectral distribution of light that can be observed remotely. - Apparent optical properties (AOP) Optical properties which depend primarily on the medium itself but have a small dependence on the ambient light field. Typically, AOPs are derived from measurements of the ambient light field, particularly upwelling and downwelling radiance and irradiance. Principal AOPs include irradiance reflectance, remote sensing reflectance, and the diffuse attenuation coefficients. - Backscattering, b_b (λ) Light of a particular wavelength (λ) that is scattered in a direction 90-180° away from its original path (i.e., backward hemisphere). Backscattered light is what is measured as ocean color in remote sensing, namely, downward propagating sunlight that has been redirected back toward the sea surface and out into the atmosphere. For natural waters, only a few percent of the light entering the ocean is backscattered out. - Colored or chromophoric dissolved organic material (CDOM) CDOM is yellow-brown in color and absorbs primarily ultraviolet and blue light decreasing exponentially with increasing wavelength. Produced from the decay of plant material, it consists mainly of humic and fulvic acids and is operationally defined as substances that pass though a 0.2 μm filter. - Diffraction Light which propagates or bends along the boundary of two different mediums with different indices of refraction. - Diffuse attenuation coefficient, K(λ) A normalized depth derivative that describes the rate of change of light, plane incident irradiance, with depth. Sunlight underwater typically decreases exponentially with depth. - Index of refraction (real), n The speed of light in a medium, c_{med}, relative to the speed of light in a vacuum, c_v expressed as n = c_v / c_{med}. The real index of refraction determines the scattering of light at the boundary between two different mediums and within the medium from thermal and molecular fluctuations. The relative refractive index, n′, is the ratio of the speed of light within the medium, c_m, to the speed of light within a particle, c_p. As n′ deviates from 1, the scattering caused by the particle increases for a general size and shape particle (e.g., minerals and bubbles). - Inherent optical properties (IOP) Optical properties which depend on the medium itself and are independent of the ambient light field. IOPs are defined from a parallel beam of light incident on a thin layer of the medium. Two fundamental IOPs are the absorption (a) and the volume scattering coefficient (β), which describe how light is either absorbed or directionally scattered by ocean water. - Irradiance (downward planar), E_d (λ) The incremental amount of radiant energy per unit time (W) incident on the sensor area (m^{-2}) from all solid angles contained in the upper hemisphere, expressed per unit wavelength of light (λ, nm^{-1}). This is used to measure the amount of spectral energy from the sun reaching the sea surface. - Irradiance reflectance, R(λ) The ratio of the upwelling irradiance, E_u (λ), to the plane downwelling irradiance, E_d (λ), in different wavelengths (λ). - Optical depth, ζ A measure of how opaque a medium is to radiation. The optical depth is a function of the geometric depth and the vertical attenuation coefficient. - Optically shallow waters An aquatic system where the spectral reflectance off the bottom contributes to radiance measured above the sea surface and is defined by the water clarity, bottom depth, and bottom composition. - Photosynthetically available radiation (PAR) The integrated photon flux (photons per second per square meter) within the 400-700 nm wavelength range at the ocean surface. PAR is the total energy available to phytoplankton for photosynthesis and is reported in units of Q m^{-2} s^{-1}, where Q is quanta, or in μE m^{-2} s^{-1}, where E is Einsteins. - Radiance, L(λ) The incremental amount of radiant energy per unit time (in Watts) incident on the sensor area (m^{-2}) in a solid angle view (sr^{-1}) per unit wavelength (λ) of light (nm^{-1}). A satellite measures radiance. - Reflection At the boundary of two different mediums with different indices of refraction, a certain amount of radiation is returned at an angle equal to the angle of incidence. - Refraction The direction of light propagation changes, or is bent, at the boundary between two mediums with different indices of refraction. The refracted light bends toward the normal boundary when the index of refraction increases from one medium to another and away from the normal boundary when the index of refraction decreases from one medium to another. - Remote sensing reflectance, R_{rs}(λ) A specialized ratio used for remote sensing purposes formulated as the ratio of the spectral water-leaving radiance, L_w (λ), to the plane irradiance incident on the water, E_d (λ). It represents the spectral distribution of sunlight penetrating the sea surface that is backscattered out again and potentially measured remotely. Theoretically, it is proportional to spectral backscattering b_b (λ) and inversely proportional to absorption a(λ) of the surface water column. - Water-leaving radiance, L_w (λ) The component of the radiance signal

measured above the water consisting of photons that have penetrated the water column and been backscattered out through the air-sea interface. It does not include photons reflected off the sea surface, also called sun glint.

Definition of the Subject, Relevance, Motivation

The oceans cover over 70% of the earth's surface and the life inhabiting the oceans play an important role in shaping the earth's climate. Phytoplankton , the microscopic organisms in the surface ocean, are responsible for half of the photosynthesis on the planet. These organisms at the base of the food web take up light and carbon dioxide and fix carbon into biological structures releasing oxygen. Estimating the amount of microscopic phytoplankton and their associated primary productivity over the vast expanses of the ocean is extremely challenging from ships. However, as phytoplankton take up light for photosynthesis, they change the color of the surface ocean from blue to green. Such shifts in ocean color can be measured from sensors placed high above the sea on satellites or aircraft and is called "ocean color remote sensing ." In open ocean waters, the ocean color is predominantly driven by the phytoplankton concentration and ocean color remote sensing has been used to estimate the amount of chlorophyll a, the primary light-absorbing pigment in all phytoplankton. For the last few decades, satellite data have been used to estimate large-scale patterns of chlorophyll and to model primary productivity across the global ocean from daily to interannual timescales. Such global estimates of chlorophyll and primary productivity have been integrated into climate models and illustrate the important feedbacks between ocean life and global climate processes. In coastal and estuarine systems, ocean color is significantly influenced by other light-absorbing and light-scattering components besides phytoplankton. New approaches have been developed to evaluate the ocean color in relationship to colored dissolved organic matter, suspended sediments, and even to characterize the bathymetry and composition of the seafloor in optically shallow waters. Ocean color measurements are increasingly being used for environmental monitoring of harmful algal blooms, critical coastal habitats (e.g., seagrasses, kelps), eutrophication processes, oil spills, and a variety of hazards in the coastal zone.

Introduction

Remote sensing of ocean color allows for the estimation of phytoplankton biomass and carbon fixation over the global ocean. From these data, approximately half of the global carbon fixation is estimated to occur by ocean phytoplankton, accounting for roughly 50 Gt C year^{-1} [1, 2]. Phytoplankton are the base of the marine food web, responsible for producing organic carbon from carbon dioxide. The premise behind ocean color remote sensing is to relate the intensity and spectral distribution of visible light reflected out of the water ("ocean color") to the biological and biogeochemical processes that influence the optical properties of the water column ("bio-optical properties") [3]. The distribution, abundance, and temporal variation in various biological, physical, and chemical processes can be observed synoptically from local and regional to global spatial scales from sensors placed on satellites or aircraft. Ocean color remote sensing provides the long-term, continuous time series of phytoplankton biomass and productivity data necessary for global carbon cycle and climate research [4-6], but the uses of ocean color data are increasingly diverse from military to environmental monitoring applications [7].

Phytoplankton have a marked influence on the subsurface and emergent light field [8]. The light harvesting systems of phytoplankton, including the chlorophyll a pigment which is ubiquitous among phytoplankton species, absorb light across the visible spectrum and influence the color of the near-surface ocean [9]. An increase in absorption, or reduction in reflectance, in the blue relative to the green portion of the spectrum can be empirically related to chlorophyll a concentration [10]. In other words, as phytoplankton are added to the water column, more blue light is absorbed and the reflected color changes from blue to green. The advent of space-based ocean color sensors in 1978 with NASA's Coastal Zone Color Scanner (CZCS) and the follow on Sea-viewing Wide Field of View Sensor (SeaWiFS) in 1997 greatly enhanced the understanding of phytoplankton distribution and concentration in the ocean [11]. Satellite ocean color imagery provides estimates of phytoplankton abundance across all ocean basins (Atlantic, Pacific, Indian, Arctic, and Southern Oceans) and quantifies the variability from seasonal to interannual timescales.

Over the last several decades, ocean color has expanded beyond chlorophyll and a whole field has emerged to study how the nature of the upwelling light field changes as a function of the quantity and composition of a variety of constituents in the near-surface ocean, including biogenic and nonbiogenic inorganic material, nonliving and living organic material (i.e., phytoplankton, bacteria and viruses), dissolved substances, and benthic habitats. Ocean color research has sought to define the fundamental relationship between the inherent optical properties of the ocean, or the absorption and

scattering properties of the constituents, and water-leaving radiance. With improved technology, including radiometers with better spectral resolution, calibration, and a high signal-to-noise ratio, and in situ optical instrumentation, which provided a description of the optical properties of oceanic constituents, biogeochemical parameters are being estimated with greater accuracy and precision. Ocean color remote sensing has moved beyond estimations of chlorophyll alone and is now used to measure total suspended sediment, colored dissolved organic material, particulate inorganic carbon, and phytoplankton functional groups, as well as critical habitats and hazards influencing pelagic and coastal waters.

Optical Properties of the Water Column

Scattering and absorption of photons, the basic unit of light energy, in the surface ocean determines the intensity and spectral shape of the water-leaving light signal measured at an ocean color sensor. Photons that propagate into the ocean interact with water molecules, dissolved and particulate matter and are either absorbed or scattered. Because most of the light is propagated downward into the water column, only a small amount of the signal is scattered back out of the water column and measured remotely. The bulk optical properties of water are used to describe how the spectral and directional distribution of photons is altered within the natural water body.

Inherent Optical Properties

The absorption and scattering properties of water molecules and the dissolved and particulate constituents within the water are called inherent optical properties (IOPs) . IOPs do not depend on the ambient light conditions, but are a function of the medium alone. The two IOPs commonly used for remote sensing purposes include the absorption (a) and scattering (b) coefficients, which refer to the fraction of incident light, a single, narrow, collimated beam of photons, which is absorbed or scattered per unit distance within the medium (units 1/length or m^{-1}). The scattering coefficient stems from the volume scattering function (β), which is the differential scattering cross section per unit volume per solid angle, and is calculated as the integral over all directions (0-180°). The attenuation coefficient (c) accounts for the reduction in light intensity due to absorption and scattering processes combined.

Both absorption and scattering processes can change the color of the ocean as observed from a satellite. Oceanic constituents that are primarily responsible for absorption of photons include water molecules, phytoplankton pigments, particulate detritus, and colored or chromophoric dissolved organic material (CDOM) (Fig. 1). Pure water is increasingly effective at absorbing light at wavelengths greater than 550 nm and absorbs minimally in the blue and green portion of the visible spectrum. Conversely, CDOM, operationally defined as all of the colored material that passes through a 0.2 μm filter, absorbs maximally in the ultraviolet and blue portion of the spectrum, decreasing exponentially with wavelength at a rate which is related to the composition, or degradation state, of the material. CDOM is generally comprised of humic and fulvic acids and small colloidal material released through the degradation of plant tissue, whether in soils or in water [12, 13]. Commonly, CDOM is modeled with an exponential function, but a hyperbolic model may be more accurate [14]. Nonliving particulate material, called detritus or tripton, absorbs in a manner similar to CDOM and the two components are difficult to differentiate spectrally.
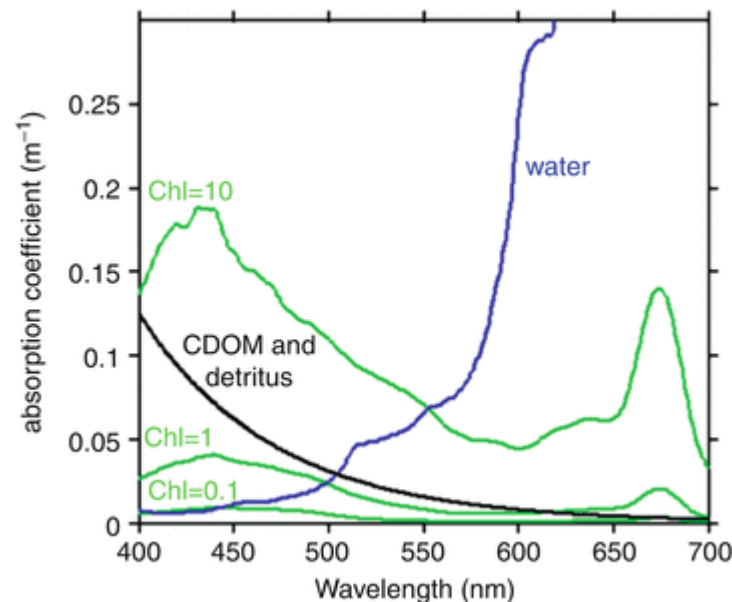
Remote Sensing of Ocean Color. Figure 1 Absorption spectrum for different constituents in seawater including water molecules, chromophoric dissolved organic matter and detritus, and phytoplankton contributions bio-optically modeled for chlorophyll at 0.1, 1 and 10 mg m^{-3} [16]

Phytoplankton absorb light in a complex manner related to the composition and quantity of their photosynthetic pigments, molecules structured to absorb photons within the visible range of 400-700 nm, dubbed photosynthetically available radiation or PAR. There are three distinct classes of pigments, namely, chlorophylls, carotenoids, and biliproteins [101]. All phytoplankton contain chlorophyll a and most contain chlorophylls b and/or c. Chlorophylls a, b, and c have two strong absorption bands in the red and blue portions of the spectrum. Chlorophyll a absorption is low in the green (450-650 nm) portion of the spectrum. The presence of chlorophylls b and c extend the range of light available for photosynthesis further into both the short- and regions. Carotenoids, of which there are many types, have both light harvesting and photoprotective functions. Finally, some phytoplankton contain red or blue pigments called biliproteins, which are divided into classes based on the position of their absorption peaks. The phytoplankton absorption coefficient describes the spectral absorption for natural waters comprised of mixtures of phytoplankton and has been commonly parameterized by chlorophyll concentration and dominant cell size [15, 16].

Scattering processes, which include refraction, reflection and diffraction, occur at the boundary of a particle with a different index of refraction , the ratio of the speed of light in the surrounding medium to the speed of light within the particle, than the surrounding medium. Scattering is predominantly elastic, the energy of the photon is conserved, but the direction of propagation is altered. Rather than reducing light, scattering works to inhibit the straight-path vertical penetration of light. The total scattering coefficient (b) can be subdivided into light which scatters in the forward direction (b_f) (0-90°) and the backward direction (b_b) (90-180°) relative to the unattenuated beam. The backscattered light is the radiance that is scattered out of the water column and measured by a sensor as "ocean color." The magnitude of b_b is a function of the concentration, composition (i.e., index of refraction), shape, and size of particles [17].

Water molecules, salts, organic and inorganic particles, and bubbles provide strong contributions to light scattering in the ocean. Scattering by pure water is the result of density fluctuations from the random motion of water molecules and has a wavelength dependence of λ^{-4} [18]. The presence of salt increases scattering, where pure seawater, with a salinity of 35-38‰, scatters 30% more light than pure water devoid of salt. When particles are present, as in natural waters, scattering increases markedly [19]. The scattering coefficient for the clearest surface waters is an order of magnitude greater than that of pure seawater. Particles that are large relative to the wavelength of light scatter mainly in the forward direction via diffraction, where photons propagating along the particle boundary change their direction in response to the boundary in a manner proportional to the cross-sectional area of the particle. Photons entering large particles are likely absorbed. Conversely, small particles mainly reflect and refract light in a manner proportional to the volume of the particle. Small particles with an index of refraction that deviates markedly from 1, including micron (10^{-6} m)-sized calcium

carbonate plates or coccoliths generated by coccolithophorid phytoplankton (n′ = 1.25) or bubbles (n′ = 0.75), are highly efficient at scattering light in the backward direction [17].

The processes of absorption and scattering are considered additive, therefore the sum of the contribution of each constituent determines the magnitude of the total coefficients a_t and b_t. As such, IOPs are separated into operationally defined components which comprise a and b_b :

$$a_t = a_w + a_{ph} + a_d + a_g, \text{ and}$$
$$b_{bt} = b_{bw} + b_{bp}$$

where the subscripts correspond to water (w), algal or phytoplanktonic (ph), non-algal or detrital (d) matter, and dissolved material, originally termed "gelbstoff" (g). Dissolved material does not scatter light and the contributions of both algal and non-algal matter are generally consolidated into backscattering from particulate (p) material. Recent advances in optical instrumentation have allowed for the measurement of absorption and scattering properties in situ and contributed to advances in ocean color remote sensing [20].

Apparent Optical Properties

Measurements of how light of different wavelengths attenuates with depth in the water column have been the historical basis of optical oceanography [21] following from the use of white Secchi disks to estimate water clarity. The properties that can be derived from measurements of ambient light in the water column are generally termed "apparent" optical properties (AOP) because they operate as optical properties describing the fundamental properties of the medium with only a slight dependence on the angular distribution of the light field. Spectral radiance, L, is the fundamental radiometric quantity which describes the spatial, temporal, directional, and wavelength-dependent structure of the light field in units of radiant flux per area per wavelength per solid angle (W m^{-2} nm^{-1} sr^{-1}) [18]. Planar downwelling irradiance, E_d, is a measure of the radiant energy flux incident on the surface from all directions or solid angles contained in the upper hemisphere, with units of radiant flux per unit area per unit wavelength (W m^{-2} nm^{-1}). The same concept, applied to the lower hemisphere, describes upwelling irradiance, E_u. The ratio of the upwelling to downwelling irradiance yields irradiance reflectance , R, a measure of how much light of a certain wavelength entering the ocean is scattered backward by ocean molecules and particles.

For remote sensing purposes, only the radiance from a specific direction is measured by a sensor, not the entire upwelling irradiance. Hence, the color is parameterized as remote sensing reflectance (R_{rs} , sr^{-1}), which is the ratio of water-leaving radiance to downwelling irradiance. The term "water-leaving radiance " represents the radiance signal emerging from the water column in a nadir direction and specifically excludes those upward-directed photons that have only reflected off the sea surface and not penetrated the water column (i.e., sun glint). The term R_{rs} represents the proportion of the downwelling light incident on the water surface that is returned through the air-water interface in the nadir direction due to differential absorption and scattering processes. The parameter R_{rs} is proportional to backscattering coefficient and inversely proportional to absorption coefficient and can be approximated as:

$$R_{rs} = \frac{f}{Q} \frac{b_b}{(a + b_b)}$$

where the ratio f/Q is related to the bidirectionality of the light field and varies from 0.09 to 0.11 for most remote sensing applications [22].

The rate of change of radiance and irradiance with depth, known as the vertical diffuse attenuation coefficient (K; m^{-1}), is another principle AOP. Irradiance and radiance decrease approximately exponentially with depth. The downward diffuse attenuation coefficient, K_d, the rate of decrease in downwelling irradiance, E_d (0), with depth (z),

$$E_d(z) = E_d(0) e^{-K_d z}$$

is commonly used in biological studies and is closely linked to the absorption coefficient of the medium specifically. The

optical depth, ζ, corresponding to any given physical depth is defined below:

$$\zeta = K_d z$$

Optical depths frequently used by biologists include 2.3 and 4.6, corresponding to the 10% and 1% light levels, respectively. Also, the portion of the surface water column contributing 90% of the water-leaving radiance has a depth, z, described by z = 1 / K_d [12]. The radiative transfer equation is the mathematical formulation that defines the relationship between the apparent and inherent optical properties of natural water bodies [18] and is the basis for the semi-analytical models used in ocean remote sensing.

Basics of Ocean Color Remote Sensing

Many challenges are inherent to remote sensing of ocean color. In comparison to land, the ocean target is dark, with an albedo of only a few percent. This means that most of the light that enters the water is propagated downward into the water column and only a few percent is scattered back out again. This is quite different from land and ice surfaces which have a much higher albedo. Most ocean color sensors are passive in that they measure only the radiation that originates from the sun, as opposed to active sensors that produce and sense their own stream of light (e.g., Light Detection and Ranging or LIDAR). Viewed from space, moreover, the ocean is observed through a thick atmosphere which reflects sunlight back to the sensor and is significantly brighter in the visible wavelengths than the water itself. In technical terms, this is quantified as a low signal-to-noise ratio where the "signal" is the light reflected from within the ocean and the "noise" is light reflected from the atmosphere and sea surface. This section outlines the platforms, calibration, atmospheric correction, and levels of data processing critical for successful ocean color remote sensing.

Sensors and Platforms

Ocean color sensors can be mounted on space-based satellites or on suborbital platforms like aircraft or unmanned aerial vehicles. The spatial and temporal sampling and the questions that can be addressed with the data depend on the type of platform employed. Most current ocean color sensors have a wide field of view, which translates to a wide sampling swath, and are mounted on sun synchronous polar-orbiting satellites (e.g., CZCS, SeaWiFS, MODIS Aqua and Terra). These sensors have the potential to provide global coverage of the earth roughly every 3 days at the equator and more frequently at the poles. However, clouds obscure the ability of the sensor to view the ocean color and, in reality, temporal sampling for any given region is much less. Data are frequently averaged over longer time periods to produce weekly, monthly, and seasonal composite images of the global ocean (Fig. 2). The spatial resolution is also limited nominally to 1 km pixel widths (and down to 250 m for select channels) in these polar-orbiting sensors in part because of limitations in signal-to-noise inherent to the dark ocean surfaces (see atmosphere correction below). Global datasets are often aggregated to 4-km or 9-km pixels. However, higher spatial resolution on the scale of meters can be obtained from some space-based platforms and from ocean color sensors placed on aircraft (Fig. 3).
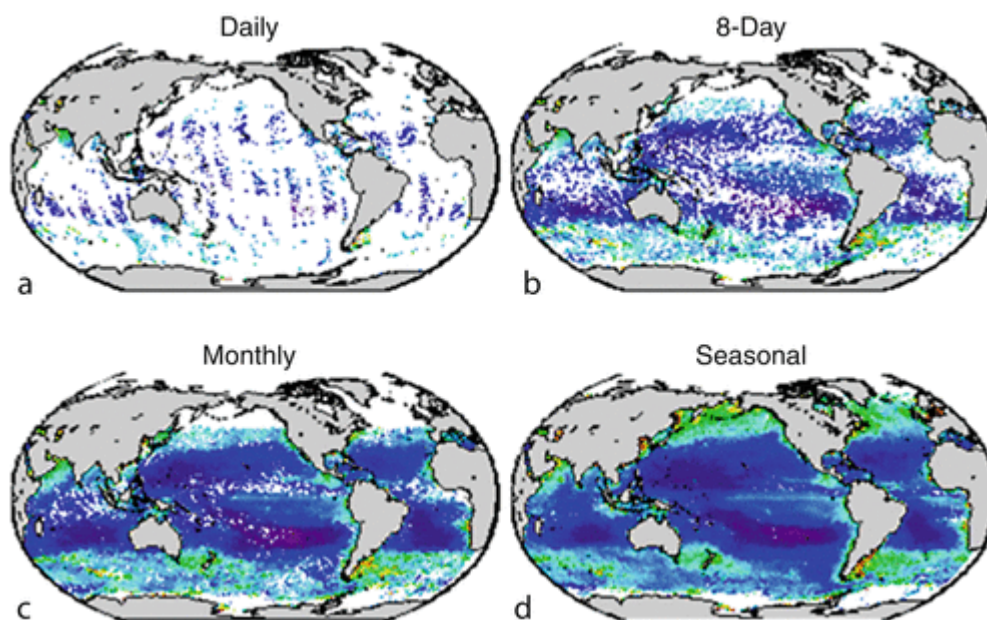
Remote Sensing of Ocean Color. Figure 2 Global maps of satellite-derived chlorophyll showing increasing levels of temporal resolution from daily to seasonal. Imagery from MODIS Aqua satellite from 2006: (a) 17 December; (b) 11-17 December; (c) 1-31 December; (d) Autumn. White spacing in imagery represents gaps in orbital coverage (daily image), as well as clouds and ice cover. Merging of imagery from different sensors can provide enhanced daily coverage [100]
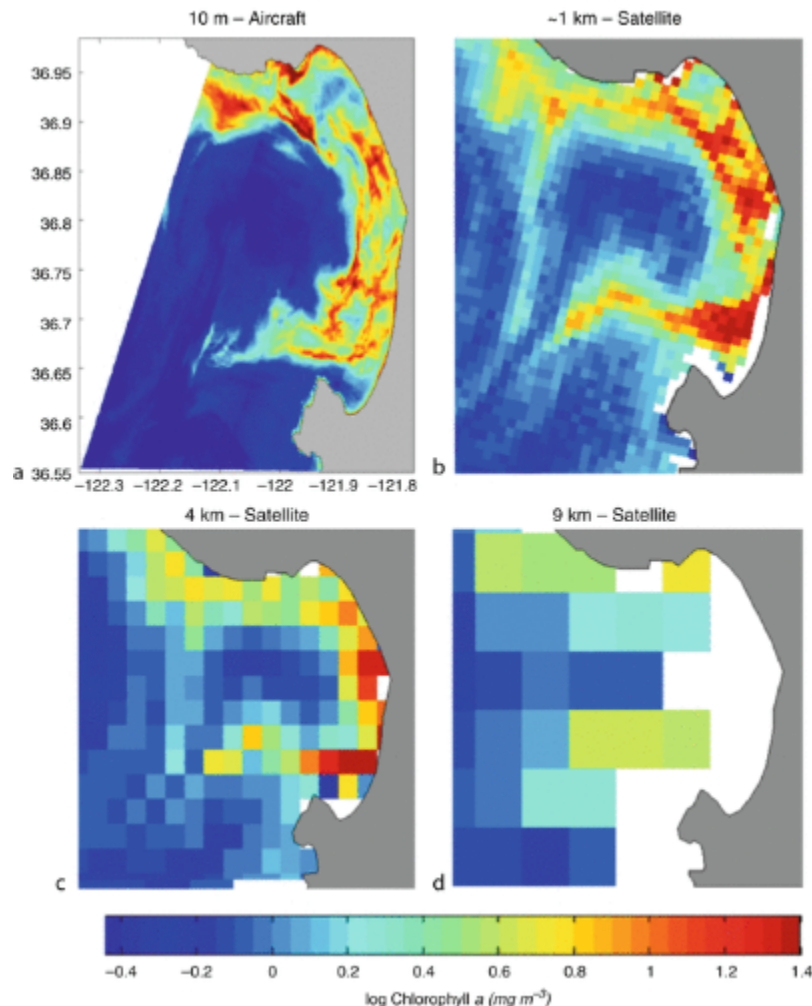
Remote Sensing of Ocean Color. Figure 3 Ocean color remote sensing imagery of Monterey Bay, California, illustrates different spatial resolutions available: (a) AVIRIS sensor flown on an aircraft, 10 m pixels [25]; (b) SeaWiFS satellite Level 2 data, 1 km pixels; (c) SeaWiFS satellite gridded to 4-km pixels; (d) SeaWiFS satellite Level 3 9-km standard product

The current suite of ocean color sensors has nominally six to seven spectral bands spanning the visible wavelengths (400-700 nm). These bands are not spread uniformly across the visible spectrum, but have been selected to correspond to reflectance characteristics of open ocean waters, particularly those related to phytoplankton pigment absorption features . Three bands are generally found in the "blue" (near 410, 440, and 490 nm), one to two bands in the "green" (510 or 530, 560 nm), and one to two channels in the "red" (670, 680 nm). In addition, channels are also incorporated in the near infrared (NIR) to short-wave infrared (SWIR) for purposes of atmospheric correction (see section "Atmospheric Correction"). Most of the visible channels were selected to match absorption features of phytoplankton and other constituents. Additional channels are also needed to bridge the large 100 nm gap between 560 and 670 nm, where absorption features are dominated by water, to better constrain backscattering in complex coastal waters [23, 24]. New technology has allowed for the development of sensors that span the full range of visible and near infrared (NIR) spectrum or "hyperpsectral," also referred to as imaging spectrometers.

No single platform is ideal for addressing all of the temporal and spatial variability in the oceans. A constellation of ocean color imagers with complementary capabilities and specifications is ultimately required to adequately address the diverse requirements of the coastal research and applied user communities. For example, the Hyperspectral Imager for the Coastal Ocean (HICO) was recently installed on the International Space Station for the study of the coastal ocean and adjacent lands. This imaging spectrometer is intended to provide hyperspectral imagery at 100-m resolution sampling at different angles and times of the day for selected regions. Sensors are also being considered for placement on geostationary satellites, similar to the international constellation of meteorological satellites. Such sensors would look at the same regional location on earth for extended periods of time and be able to provide better temporal resolution of

ocean processes and episodic hazards. Regional efforts such as the Geostationary Ocean Color Imager (GOCI) on the COMS-1 platform from South Korea are already planned for launch. In addition, higher spatial and spectral resolution polar orbiting sensors are proposed to address questions related to seasonal variability in global coastal habitats and polar ice cover.

Portable sensors flown on aircraft or unmanned aerial vehicles (UAV's) provide a critical sampling niche distinct from satellite-borne sensors that is particularly well suited for coastal applications and ice research (Fig. 3a) [25]. Airborne sensors can sample at finer spatial scales (meters), can operate under clouds and with nearly unlimited repeat coverage, and are effective platforms for high-resolution active sensors (e.g., LIDAR). Flight lines and scanning geometries can also be oriented to avoid sun glint and their range can be greatly expanded by launching from ships. The technology required to build portable sensors for coastal applications is developing with wide field of views, minimum polarization dependence, high response uniformity, and optimized signal-to-noise ratio for low-light channels [26, 27]. These sensors are becoming more popular for use in the environmental management of coral reefs, seagrasses, kelps, and other coastal targets, and have the potential to monitor episodic events such as harmful algal blooms and runoff and flooding from storms.

Ocean color sensors in space have traditionally been "whisk broom" in design where a single detector collects data one pixel at a time as the telescope rotates to build up pixels along a scan line. Some satellites and most of the suborbital sensors are "pushbroom" where the entire scan line is imaged synoptically by a line of sensors arranged perpendicularly to the flight direction. In order to achieve high-quality data that can track climatological trends in ocean color, sensors are required to have very high radiometric accuracy and stability. Detectors are calibrated pre- and post-launch and degradation over time is carefully quantified with vicarious calibrations from field measurements and ideally lunar imaging. Periodic reprocessing of the satellite data is considered critical to obtaining high-quality datasets and continuity over multiple missions [5, 28].

Atmospheric Correction

One of the most challenging aspects of ocean color remote sensing is successfully removing the atmospheric signal from the water column signal. Aerosols and gas molecules are the primary contributors to the radiance measured at the top of the atmosphere. Approximately 80-85% of the radiance measured at the sensor is the result of Rayleigh scattering by molecules in the atmosphere that are small relative to the wavelength of light. Photons reaching the sensor (L_u) are a combination of those scattered by the atmosphere (L_p), reflected at the air-water interface (L_r), known as specular reflection, or have been backscattered from within the water column, dubbed water leaving radiance, or L_w (Fig. 4). The water-leaving radiance, used for most ocean color applications, is only a small portion of the signal retrieved at a satellite and must be differentiated from the photons scattered within the atmosphere and specularly from the sea surface in a process called "atmospheric correction."
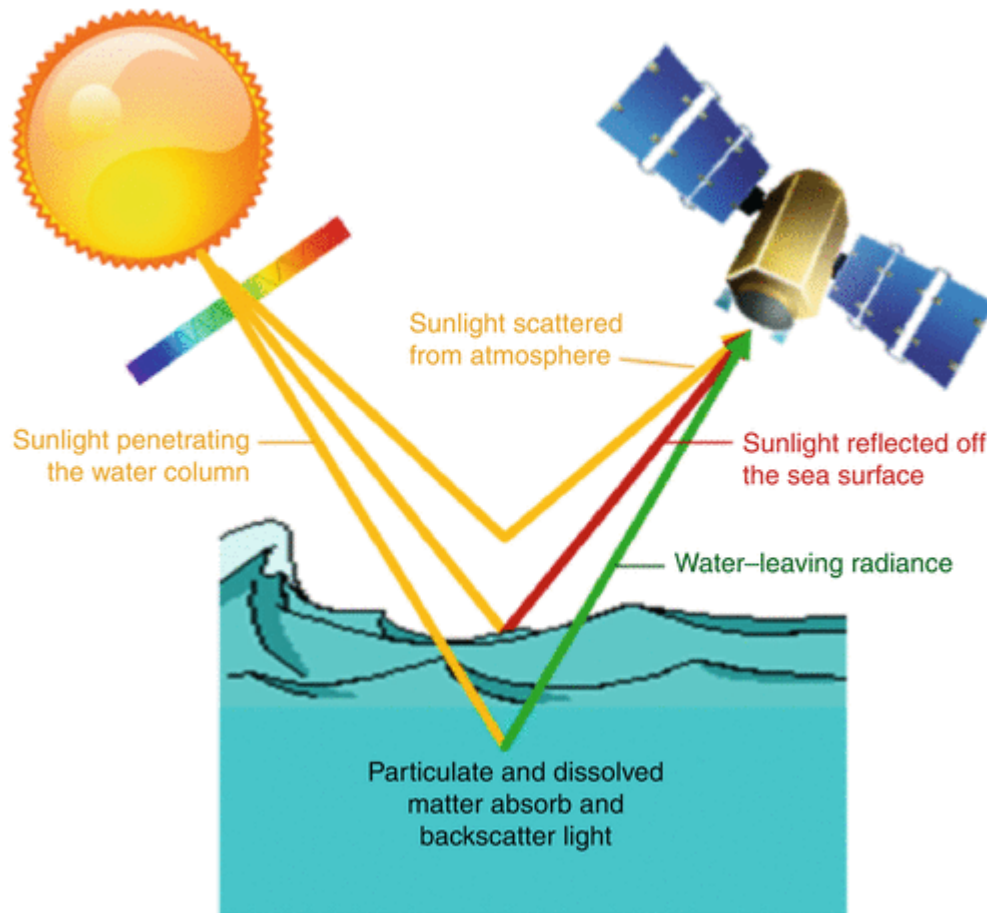
Remote Sensing of Ocean Color. Figure 4 Radiance measured by a satellite includes light scattered by the atmosphere and reflected off the sea surface (i.e., glint). In a process called "atmospheric correction," these signals are removed leaving the "water-leaving radiance" or the light that has penetrated the water column and been backscattered out to the satellite - a measure of ocean color

Rayleigh scattering , which decreases with wavelength (λ) following λ^{-4}, can be estimated using a single-scattering radiative transfer equation using the atmospheric pressure and appropriate viewing geometry [29]. An additional 0-10% of the radiance signal is due to aerosols (i.e., haze, dust, and pollution), particles with sizes comparable to the wavelength of light which absorb and scatter as a complex function of their type, size, and concentration. The type and concentrations of aerosols overlying the ocean are quite variable in space and time, particularly in coastal regions subject to urban pollution and terrestrial dust [30].

Atmospheric correction of aerosols remains a challenge for accurately deriving water-leaving radiance from satellites and aircraft. Approaches generally focus on channels in the NIR and even in the short wave infrared (SWIR) [29, 31, 32]. Because water absorbs so heavily in the infrared, very few photons are reflected out of water in this part of the electromagnetic spectrum and the signal is dominated by reflection from atmospheric gases and aerosols. Various types of models are used, including coupled models and multi-scattering models, to infer the contribution of aerosol reflectance in the visible portion of the spectrum from the infrared. Aerosol reflectance is not spectrally flat, but varies with wavelength, and at least two channels are necessary to determine the spectral shape of aerosol reflectance and extrapolate from the NIR to visible wavelengths [29, 33].

Dust, particularly from desert storms, can also impact the optical properties of the atmosphere and most atmospheric correction algorithms for ocean color sensors are not capable of handling absorbing mineral dust (i.e., colored dust) [34]. For example, airborne plumes of Saharan dust are observable all year on satellite images over the Tropical Atlantic and may be increasing in areas like the Mediterranean Sea [35]. If colored dusts are not properly corrected for in the atmospheric correction schemes, then the color of the ocean is not accurately estimated resulting in errors in chlorophyll

and other biogeochemical properties retrieved from the satellite data [36]. In addition to its radiative impact, it has been suggested that this mineral dust has a substantial influence on the marine productivity and may also carry pollutants to the oceans [37, 38].

Whitecaps breaking on the sea surface must also be corrected from derivations of water-leaving radiance. Whitecap reflectance is often modeled using an empirical cubic relationship to wind speed and an approximate reflectance value for an individual whitecap [39], but such models often overcorrected the imagery, and a fixed whitecap correction is applied when wind speeds exceed a threshold (e.g., 8 m s^{-1} for SeaWiFS). At high winds, some of the signal attributable to whitecaps is removed by the aerosol corrections.

Levels of Processing

Standards for ocean color data processing, developed at US National Aeronautics and Space Administration (NASA) for the SeaWiFS mission [40], are widely followed by the international community of ocean color users and involve four levels of processing (Table 1).

Remote Sensing of Ocean Color. Table 1 Levels of data processing products from ocean color satellites

Level	Processing	Spatial qualities
0	Raw data as measured directly from the spacecraft	Satellite coordinates at highest spatial resolution
1	Converted to radiance using calibrations and sensor characterization information	Satellite coordinates at highest spatial resolution
2	Atmospherically corrected to water-leaving radiance and derived products	Satellite coordinates at highest spatial resolution
3	Derived products have been mapped onto a two-dimensional grid at known spatial resolution and can be averaged over timescales (weekly, monthly)	Regular gridded data at lower spatial resolution (e.g., 4 or 9 km)
4	Products that have been merged or assimilated with data from other sensors, in situ observations, or model outputs	Regular gridded data at lower spatial resolution

Ocean Color Algorithms

This section presents the classification of the global ocean into two optical classes: Case 1 and Case 2. The general approaches for two of the main products from ocean color imagery, chlorophyll and primary productivity, for Case 1 waters and a description of the semi-analytical algorithms used for both Case 1 and Case 2 waters are presented.

Optical Classification of Aquatic Systems

Ocean waters have long been classified based on their color properties [41]. A classification system introduced in 1977 differentiates phytoplankton-dominated waters from those where inorganic particles are dominant, known as Case 1 and Case 2, respectively [42]. These cases have evolved from their original forms into the categories used today: Case 1 waters are those waters where optical properties are determined primarily by phytoplankton and related colored dissolved organic matter (CDOM) and detritus degradation products; Case 2 waters are waters where optical properties are significantly influenced by other constituents such as mineral particles, CDOM, or microbubbles that do not covary with the phytoplankton concentration [8, 43]. In today's world, approximately 97% of the surface ocean falls toward the optically simple, deep water, Case 1 classification. When inorganic, organic, particulate, and dissolved material all vary independently of one another, such as in coastal ecosystems with considerable riverine influence, bottom resuspension, or optically shallow regions, the system falls toward the Case 2 classification, also called "optically complex."

This binary classification scheme has been prevalent in bio-optical modeling of ocean waters and development of ocean color algorithms. However, many problems exist with use of such simplified schemes in modeling natural systems. For example, there is no sharp dividing line between the cases and each investigation tends to use as different criteria for defining Case 1 and Case 2. Commonly the two cases are defined by the relationship between chlorophyll and remote sensing reflectance or scattering. Even in the global ocean considered to be Case 1, CDOM concentrations do not covary with the instantaneous chlorophyll concentration [44], but can vary from 30% to 60% of the total non-water light

absorption [45] and result from differences in water mass ventilation, water column oxidative remineralization, and photobleaching [46].

In optically shallow waters, in addition to the water column and its constituents (i.e., dissolved and particulate material), the bottom contributes to the water leaving radiance in a way that depends on the bottom composition and roughness. Periodic measurements of bottom types using passive remote sensing in coastal systems are valuable for describing and monitoring habitats [47]. The magnitude and spectral quality of light reflected off of the bottom material can allow separation of bottom reflectance from the water column signal, where different bottom types will have a different effect on reflectance. Shallow, clear water will yield the most information about bottom material, more readily allowing spectral discrimination of bottom type. However, as depth and the diffuse attenuation coefficient, K_d, increase, the bottom signal becomes difficult to differentiate.

Empirical Chlorophyll Algorithms

Standard calculation of chlorophyll from ocean color imagery involves an empirical relationship developed from field observations collected throughout the global ocean [10]. Algorithms are typically not developed from the remotely sensing imagery itself, because this would incorporate any biases in calibration and atmospheric correction procedures used to derive reflectance, as well as any spatial inhomogeneity in parameters over pixel scales, and would require new algorithms for every new calibration, reprocessing, and sensor. Empirical solutions are used because an analytical solution to the problem requires an assessment of the entire radiance distribution and depth derivative and such measurements are not possible with remote sensing [48]. Only the upward flux incident upon the water-air interface at angles less than 48°, the angle at which complete internal reflection occurs, is measurable from above the sea surface [6] and generally only the flux emitted in a single viewing angle is remotely sensed.

The current empirical algorithms use the shift in ocean color from "blue" at low Chl, where R_{rs} peaks at 400 nm, to "green" at high chlorophyll, where R_{rs} peaks at 555 nm (Fig. 5a). Empirical ocean color algorithms have been applied to the vast majority of the global ocean considered Case 1 and use multiple ocean color bands typically log-transformed and in a ratio formulation to minimize problems with atmospheric correction and differential scattering in the ocean. The coefficients for the algorithms are regularly adjusted to account for different sets of wavebands in various sensors and as new field data becomes available (Table 2). The OC3M algorithm developed for MODIS, for example, uses a 4th order polynomial derived from a large global dataset of field measurements of chlorophyll and R_{rs}. It uses a logarithmic ratio of blue light (either 443 and 488 nm depending on which is greater) to green light (555 nm) and follows an inverse relationship such that low Chl is retrieved or high ratios when the ocean color is blue and high Chl when more green light is reflected (Fig. 5b). These types of algorithms tend to work best at lower Chl (<1 mg m^{-3}), found in most of the world ocean, where the algorithm has a flatter slope [49].
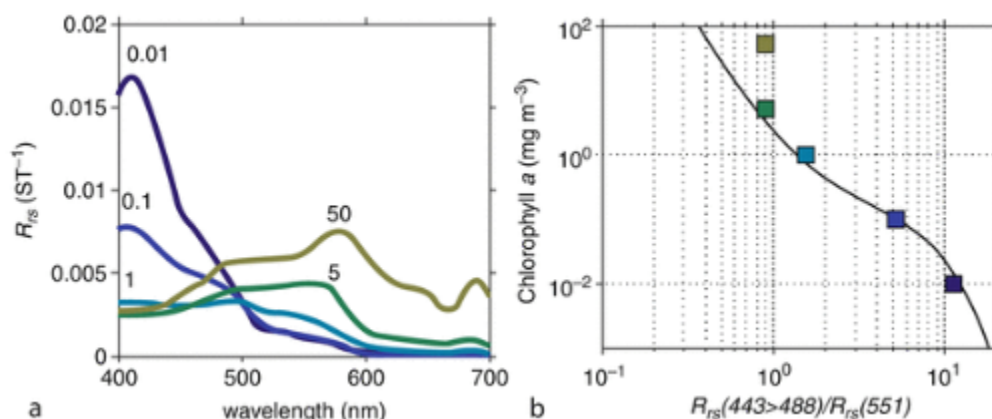
Remote Sensing of Ocean Color. Figure 5 (a) Remote sensing reflectance (R_{rs}) spectra modeled for different concentrations of chlorophyll a (Chl) from 0.01 to 50 mg m^{-3}. The color of each line represents the modeled ocean color a human might observe following [61]. (b) The empirical OC3M model for deriving Chl from R_{rs} for the MODIS Aqua sensor. The model uses the "blue" channel with the highest R_{rs} value (443 or 488 nm) divided by the "green" channel at 551 nm. Each square represents the modeled Chl for the corresponding R_{rs} spectra in panel A and demonstrates how the model becomes less accurate at high Chl

Remote Sensing of Ocean Color. Table 2 Empirical chlorophyll algorithms for a variety of ocean color sensors

Name[a]	Sensor	Channels[b]		Coefficients[c]				
		Blue	Green	a0[c]	a1	a2	a3	a4
OC4	SeaWiFS	443 > 490 > 510	555	0.366	−3.067	1.93	0.649	−1.532
OC3S	SeaWiFS	443 > 490	555	0.2409	−2.4768	1.5296	0.1061	−1.1077
OC2S	SeaWiFS	490	555	0.2372	−2.4541	1.7114	−0.3399	−2.788
OC3M	MODIS	443 > 488	551	0.283	−2.753	1.457	0.659	−1.403
OC2M	HMODIS	469	555	0.1543	−1.9764	1.0704	−0.2327	−1.1404
OC4O	OCTS	443 > 490 > 520	565	0.4006	−3.1247	3.1041	−1.4179	−0.3654
OC3O	OCTS	443 > 490	565	0.2836	−2.1982	1.0541	0.186	−0.717
OC2O	OCTS	490	565	0.2805	−2.167	1.1789	−0.1597	−1.5591
OC3C	CZCS	443 > 520	550	0.3012	−4.4988	9.0983	−9.9821	3.235

[a]Name of ocean color (OC) algorithm incorporates the number of wavebands (2-4) used in the formulation and the initial for the sensor used (S = SeaWiFS; M = MODIS; O = OCTS; C = CZCS)

[b]The algorithms use a log-transformed ratio of "Blue" (443-520 nm) to "Green" (550-565 nm) remote sensing reflectance (R_{rs}). When more than one "Blue" channel is provided, only the channel with the highest R_{rs} is used. $x = \log_{10}(R_{rs}(\text{Blue})/R_{rs}(\text{Green}))$

[c]Chlorophyll a is modeled as a fourth polynomial fit to the field data such that: $\text{Chl} = 10^{\wedge}(a0 + a1 {}^{*} x + a2 {}^{*} x^2 + a3 {}^{*} x^3 + a4 {}^{*} x^4)$

For much of the open ocean where chlorophyll concentrations are low, the empirical algorithms work well and relative error is estimated to under 35% [50]. However, empirical derivations of chlorophyll in Case 1 waters can be in error by a factor of 5 or more, particularly at higher Chl [49]. Such variability is due to differences in absorption and backscattering properties of phytoplankton and related concentrations of colored dissolved organic matter (CDOM) and minerals. The empirical algorithms have built-in assumptions that follow the basic precept of biological oceanography; i.e., oligotrophic regions with low phytoplankton biomass are populated with small phytoplankton while more productive regions contain larger bloom-forming phytoplankton . With a changing world ocean, phytoplankton composition may shift in response to altered environmental forcing and CDOM and mineral concentrations may become uncoupled from phytoplankton stocks creating further uncertainty and error in the empirical approaches [49].

The empirical approach is not widely applicable in Case 2 waters, generally found near the coasts. Such waters are influenced by freshwater plumes with CDOM and minerals that significantly impact the optical properties, as well as resuspension of bottom sediments [51]. Phytoplankton assemblages can also be diverse in coastal regimes and light absorption per unit of Chl is difficult to constrain. Melting and runoff of glacial sources can increase particle concentrations in the nearshore and change phytoplankton assemblages. In order to use remote sensing in coastal waters, semi-analytical models are employed that are able to decompose the reflected color into the many absorbing and scattering constituents in the water column (see section "Semi-analytical Algorithms").

Primary Productivity Algorithms

Net primary production is a key parameter derived from ocean color data that provides a measure of how much carbon dioxide is taken up and incorporated into ocean phytoplankton during photosynthesis. Export of fixed carbon to the ocean interior, while only a fraction of the total biomass produced, provides a long-term sink for atmospheric carbon dioxide [52]. While satellite-derived Chl is not a direct measure of carbon fixation in phytoplankton, such estimates are typically derived from correlates of Chl and rates of carbon fixation [53]. Net primary productivity varies with phytoplankton species assemblages and their physiological state related to light, temperature, nutrients, and other environmental factors.

A variety of formulations have been developed for ocean color remote sensing and parameterized for the global ocean or specific regions. Models are generally restricted to parameters that can also be globally derived from remote sensing imagery, such as sea surface temperature and photosynthetically available radiation (PAR). Moving from a standing stock of phytoplankton biomass to photosynthetic rate requires a time-dependent variable. Solar radiation in the form of PAR is

commonly used in formulations to convert biomass to primary productivity. The physiological response of the measured chlorophyll to light, nutrients, temperature, and other environmental variables must also be incorporated in the model. Primary productivity models can be differentiated by the degree of explicit resolution in depth and irradiance [53].

Round robin experiments have been conducted to compare the performance of models for assessing global productivity from ocean color imagery, as well as the output from ecosystem-based general circulation models [1, 54]. The third such effort found that global average primary productivity varied by a factor of two between models and the global mean productivity for the different model groups ranged from 44 to 57 Gt C year^{-1} with an average of 50.7 Gt C year^{-1}. The models diverged the most in the high-nutrient low chlorophyll waters of the Southern Ocean. Primary productivity algorithms have also been formulated from remote sensing estimates of the inherent optical properties (such as light absorption and backscattering) directly [55, 56], without incorporating Chl and the associated uncertainties inherent in that parameter.

Semi-analytical Algorithms

The empirical algorithms used for deriving chlorophyll have been likened to a "black box" that provides no mechanistic understanding of ocean optics and are particularly challenging to apply in a changing ocean, when the water properties are different from the empirical data used to develop the formulation [57]. Analytical solutions to deriving IOPs from water-leaving radiance are not possible because the radiance can only be measured from a few angles. Semi-analytical algorithms (or "quasi-analytical") are based on a fundamental understanding of the propagation of light in the ocean and provide a more mechanistic approach to ocean color. These algorithms incorporate some empirical approximations, but do not rely on fixed predetermined relationships between the absorption and backscattering components of the water column.

In semi-analytic models, the ocean color signal is inverted to obtain estimates of the various absorbing and backscattering constituents directly. Parameterization of how water, phytoplankton, and dissolved and detrital material inherently absorb and backscatter light across the visible spectrum (i.e., their spectral shape) is used in these models. The spectral reflectance measured at the satellite is often inverted to retrieve the amounts of each individual component contributing to the absorption and backscattering of light. Such algorithms are the primary methods for obtaining CDOM distributions across the ocean surface [58]. In semi-analytical models, the biogeochemical parameters, such as Chl and total suspended matter, are derived secondarily from the IOPs. Semi-analytical formulations vary in terms of their architecture and statistical methods employed to retrieve the inherent optical properties from the remote sensing signal and the empirical parameterizations within the models [57].

Applications for Oceanography

Ocean color remote sensing is an important tool for many branches of oceanography, including biological, physical, and chemical oceanography. The section below summarizes only some of the main applications of ocean color remote sensing with the understanding that the uses of ocean color are continuously expanding. A recent monograph from the International Ocean Color Coordinating Group (IOCCG) entitled "Why Ocean Colour?: The Societal Benefits of Ocean-Colour Technology" extensively documents the many uses of ocean color remote sensing from scientists to environmental managers to the general public [7]. Web-based software has also been developed, see, e.g., Giovanni [59], which allows the public to freely map and analyze ocean color imagery over time and space. Figure 6 provides an example of various types of figures that can be easily generated from remotely sensed chlorophyll using that software.
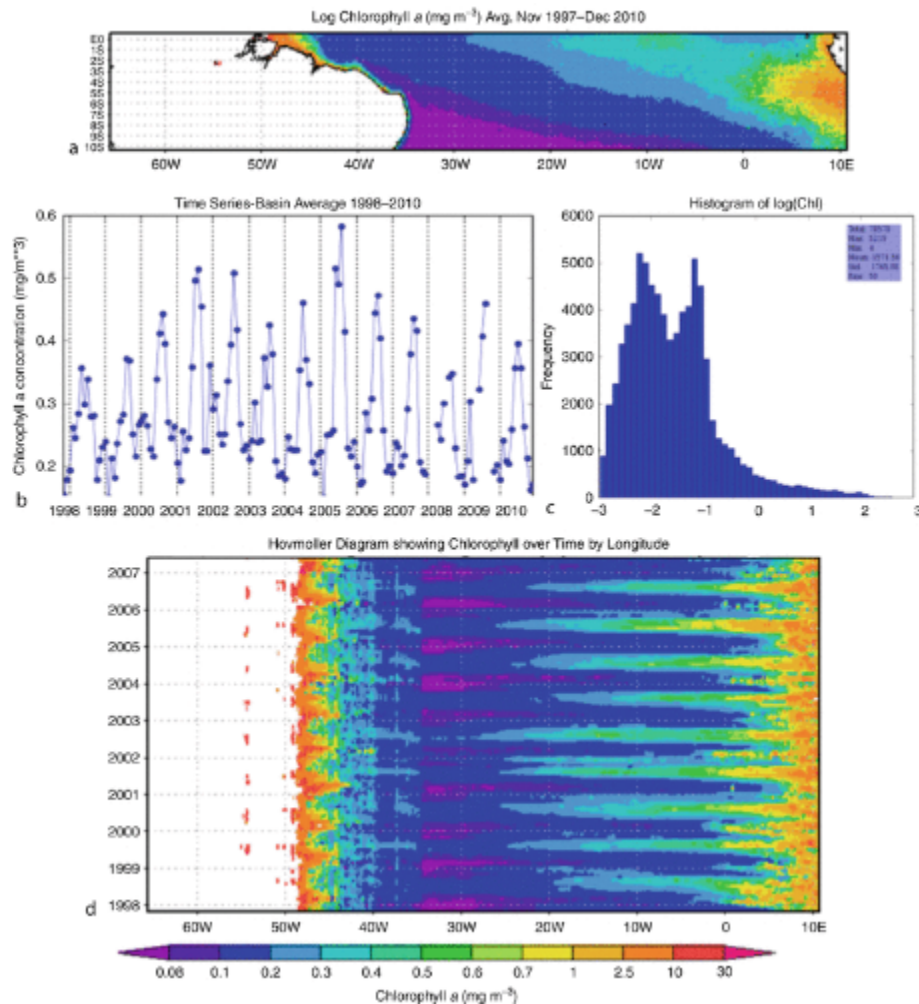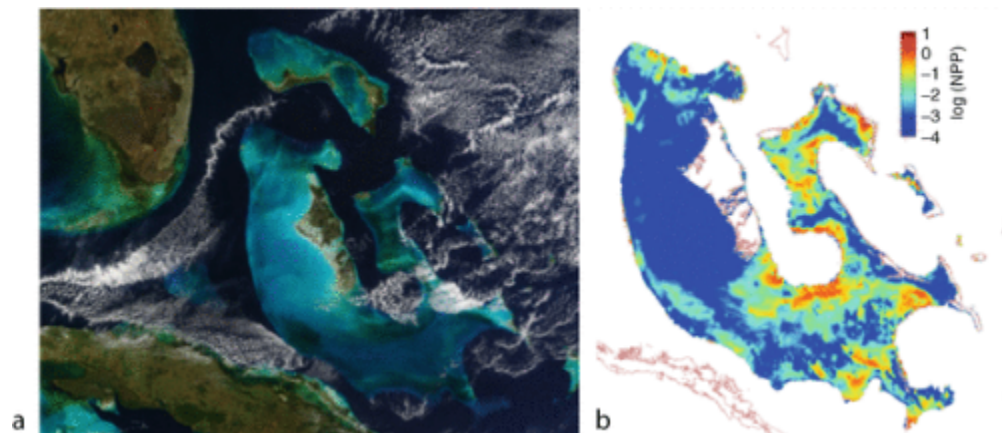
Remote Sensing of Ocean Color. Figure 6 Various times series analyses that can be conducted with standard Level 3 chlorophyll imagery including (a) Temporally averaged spatial distributions; (b) time series of interannual variability; (c) histograms showing the statistical distributions; (d) Hovmoller plots presenting both spatial (x-axis) and temporal (y-axis) variability. Such plots can be easily generated by the public with the Giovanni interface [59]

Biological Oceanography

Apart from estimating chlorophyll and primary productivity, ocean color remote sensing has many biological applications that range from phytoplankton physiology to assessing distributions of migrating whales. Phytoplankton physiology, particularly the efficiency of light capture and utilization, has been modeled from the natural fluorescence signature provided by ocean color remote sensing [60]. Even though the spectral resolution available in most current ocean color satellite is limited to six to eight available spectral channels [61], a variety of phytoplankton taxa and groups have also been distinguished from satellite imagery based on their unique optical properties and/or regional tuning of algorithms using knowledge of the local phytoplankton composition. Phytoplankton taxa can have unique sets of accessory pigments that differentiate them from one another and can result in unique absorbance spectra. In addition, phytoplankton can have cell walls or exterior plates comprised of different materials (e.g., silica, calcium carbonate) that can make them more or less reflective. Various approaches have been developed to map size classes (from pico- to microplankton) or major groups of phytoplankton in the global ocean [62]. Other algorithms have targeted particular phytoplankton taxa such as coccolithophores, nitrogen-fixing Trichodesmium [63], toxic dinoflagellates [64], and nuisance cyanobacteria [65].
Satellite-derived chlorophyll and primary productivity provide a key metric to assess marine ecosystems temporally on a global scale and have been used extensively to monitor conditions that impact other biological organisms in the sea. The relationship between satellite-derived chlorophyll data and organisms at higher trophic levels depends upon the number

of linkages in the food web. For species like anchovies and sardines, which eat phytoplankton in their life cycle, the linkage can be direct [66]; whereas, many trophic levels can exist for other species and the relationship can be quite nonlinear [7]. The distribution, movement, and migration of whales, dolphins, pinnipeds, penguins, and sea turtles has been related, either directly or indirectly, to remotely sensed patterns of Chl (reviewed in [7]). Most fish have planktonic larval stages that are strongly influenced by ocean circulation and recruitment success has been found to be related to the degree of timing between spawning and the seasonal phytoplankton bloom, as observed from satellites [67]. Ocean color remote sensing has also been used to study invertebrates in the global ocean, such as shrimp in the Newfoundland-Labrador Shelf [68] and pteropods and pelagic mollusks in the Ross Sea [69]. Mean net primary productivity, determined from ocean color satellite imagery, elucidates species richness in biogeographical studies of cephalopods [70].

New techniques have also been developed to use ocean color remote sensing in optically shallow water systems to deduce changes in benthic habitats [71]. Optically shallow water occurs when the seafloor contributes to the reflectance signal observed remotely by a satellite (Fig. 7a) and is defined by a combination of water clarity, water depth, and bottom composition. Satellite estimates of biomass and net productivity of seagrasses, kelps, and other benthic producers have been conducted over regional scales [47, 72] (Fig. 7b). Ocean color imagery from aircraft can map fine-scale distributions of seagrasses, coral reefs, and other coastal habitats at local scales [73, 74]. Changes in ocean color signals over time can also be used to assess contributions of coastal carbon to the global carbon cycle [75, 76]. Responses of coastal regions linked to terrestrial changes can also be observed with ocean color imagery. Warming of the Eurasian landmass, for example, has led to enhanced productivity in the water column [77]. Agricultural runoff from fields in Mexico was shown to stimulate large phytoplankton blooms in the Gulf of California that alter water clarity and potentially lead to anoxic conditions [78].

Remote Sensing of Ocean Color. Figure 7 The Great Bahama Bank is an example of optically shallow water where the seafloor color can be observed from space. (a) Pseudo-true color image from MODIS Aqua showing the bright Bahamas Banks with Florida, USA, to the West and Cuba to the Southwest. White wispy clouds can obscure the ocean color. (b) Net primary productivity (mgC m^{-2} d^{-1}) of seagrass and benthic algae estimated from ocean color imagery over the Great Bahama Bank [47]

Ocean Physics

Ocean color data is well suited to the detection of convergence zones and oceanic fronts, sometimes better than thermal sensors which penetrate only the skin layer, or the first 10 μm, of the water column. Interestingly, a sequence of ocean-color-derived chlorophyll images may help predict the formation of eddies days before they appear. The increased penetration of visible radiation reveals more frontal features and with greater detail than those retrieved with sea surface temperature data alone [79]. Likewise, upwelling regions, which bring cold, nutrient-rich waters up to the surface can be readily identified in ocean color images as areas with an enhanced chlorophyll concentration. The intensity of upwelling from year-to-year can be tracked through the time series of chlorophyll abundance. Chlorophyll is an effective indicator for detecting anomalous activity in the oceanic environment. Evidence of an El Niño event beginning in November of 1997, during which phytoplankton pigment concentrations appeared anomalously low in the Equatorial Upwelling Zone, was obvious in the continuous coverage supplied by SeaWiFS. The onset of restored upwelling was likewise evident with the increased chlorophyll concentrations during the months of June and July 1998 [80].

Ocean water clarity also affects the distribution of shortwave heating in the water column. Both chlorophyll and CDOM concentrations have been linked to changes in heating of surface waters [81, 82]. Increased clarity would be expected to cool the surface and heat subsurface depths as shortwave radiation penetrates deeper into the water column. Recent studies show that water clarity, as determined from ocean color remote sensing , is an important feature in atmospheric circulation (the Hadley cells), oceanic circulation (Walker Circulation), and formation of mode water [83]. Importantly, ocean color imagery is also critical to predicting tropical cyclone activity. The presence of light-absorbing constituents (like Chl and CDOM) shapes the path of Pacific tropical cyclones and propagation to higher latitudes [84].

Chemical Oceanography

A major contributor to the ocean carbon system is colored dissolved organic material (CDOM), a mixture of compounds produced primarily by decomposition of plant matter. CDOM, when present in high enough concentrations, produces a yellow or brownish color and is highly reactive in the presence of sunlight. When CDOM undergoes photodegradation, organic compounds essential to phytoplankton and bacterial growth are released [85]. Satellite measurements collected using SeaWiFS, MODIS, and MERIS produce daily estimates of CDOM at 1 km resolution. High temporal resolution CDOM maps can be used to identify and track water masses at timescales close to the processes determining its distribution. CDOM dynamics play an important role in ocean biogeochemistry, regulating the absorption of blue and UV radiation in the surface ocean and therefore altering the depth of the euphotic zone [58] and heating surface waters [82]. Although CDOM is difficult to analyze chemically, its distribution and abundance, identifiable using ocean color remote sensing, is highly relevant to understanding carbon cycling in the ocean.

The particulate inorganic carbon (PIC) pool, calcium carbonate ($CaCO_3$), contributes substantially to the ocean carbon cycle and ocean color reflectance. Calcification reduces surface carbonate, decreasing alkalinity. Organic carbon production via photosynthesis counterbalances this effect. Coccolithophores, haptophyte algae, are responsible for the majority of the biogenic particulate inorganic carbon production. Coccolithophores generate and shed tiny white plates of calcium carbonate called coccoliths, which are highly efficient at reflecting light, ultimately producing large turquoise patches in the ocean readily visible in ocean color imagery [86]. Ocean color remote sensing algorithms have been formulated for generating quantitative estimates of particulate inorganic carbon and calcification rates on regional and global scales [87, 88]. A continued, long-term assessment of coccolithophore and particulate inorganic carbon abundance from satellite imagery will aid in understanding the impact of ocean acidification on marine organisms reliant on carbonate for the formation of shells [89].

Ocean color imagery provides the ability to expand small-scale biogeochemical studies to regional or global scales. For example, the marine inorganic carbon cycle has been shown to be not only influenced by marine plankton but also by fish that precipitate carbonates into the surface waters. Extrapolations from satellite-derived net primary productivity up several trophic levels to marine fish [90] reveal that fish may contribute 3-15% of the total oceanic carbon production [91].

Applications for Environmental Monitoring

Ocean color remote sensing plays a major role in monitoring and sustaining the health and resilience of marine ecosystems, including fisheries and endangered species [40]. Ocean color products are helping to address how environmental variability influences annual recruitment of fish stock [92] and to locate and manage fisheries [7]. Ocean color imagery coupled with other remote sensing products such as sea surface temperature is a fundamental tool in ecosystem-based management of marine resources [93].

Ocean color remote sensing can monitor a variety of acute and chronic hazards influencing the oceans including: harmful algal blooms, oil spills, coastal flooding, icebergs and marine debris [7]. A combination of ocean color, field, and meteorological datasets have been critical in identifying the onset of harmful algal blooms (HABs) , which can produce toxins and create hypoxic conditions. While toxins cannot be directly observed from ocean color, the onset of potential harmful blooms can be identified using a chlorophyll anomaly method [94] in concert with other forecasting tools such as field and meteorological datasets. This information can then be passed on to coastal managers and state agencies to put strategies in place to deal with an impending bloom. A long-term time series of ocean color products can aid in elucidating forcing and transport mechanisms of these harmful blooms and help improve predictability.

New techniques are being developed for early detection, containment, and clean up of oil spills. Remote sensing can be used to detect oil spills that can change surface reflectance properties and the color of the ocean [95]. Coarse spatial and

temporal resolution, limited spectral bands, cloud-cover issues and high sunlight requirements have generally restricted the usefulness of ocean color imagery for oil-spill detection from polar orbiting satellites [96]. Moreover, current processing methods may not allow data availability within hours of data capture. The spatial,temporal, and spectral resolution needed for oil spill recovery planning requires high-resolution, hyperspectral ocean color radiometers deployed in geostationary orbit [40].

Ocean color imagery has also been used to track marine debris on the ocean surface which can entangle a variety of pelagic species, such as endangered sea turtles, seals, and whales. The nets also become ensnared on coral reefs and damage the reef structure and associated organisms that require a healthy reef ecosystem [97, 98]. Satellite ocean color data are part of the methods being developed to locate and identify potential locations of marine debris to aid their removal from these ecosystems.

Ocean color imagery is also useful in monitoring water quality in inland aquatic water bodies. Nuisance algal blooms, such as cyanobacteria, cause aesthetic degradation to lakes and reservoirs resulting in surface scum, unpleasant taste and odor in drinking water (from the production of metabolites such as methyl isoborneol and geosmin), and possible adverse effects to human health from blue-green algal toxins. Predicting the locations and timing of blue-green algal bloom using traditional sampling techniques is difficult and hyperspectral remote sensing can be an important tool in such monitoring efforts [99].

Future Directions

Within a few decades, the ability to view the global ocean color regularly through remote sensing has revolutionized the perceptions about ocean processes and feedbacks to the earth's climate. The decade of continuous ocean color imagery has provided a foundation for assessing change in the earth's systems and long-term averages or "climatologies" of products, such as chlorophyll, CDOM, and PIC, have been produced to provide a baseline of ocean biogeochemistry (Fig. 8). The products obtained from ocean color are now incorporated into all domains of oceanography, global climate forecasts, military applications, and environmental monitoring across the expansive global ocean and the vulnerable coastal regions where most of the human population resides [11]. While successful, the technology and processing of ocean color remote sensing is still in its infancy in terms of monitoring the ocean from immediate to climatological timescales.
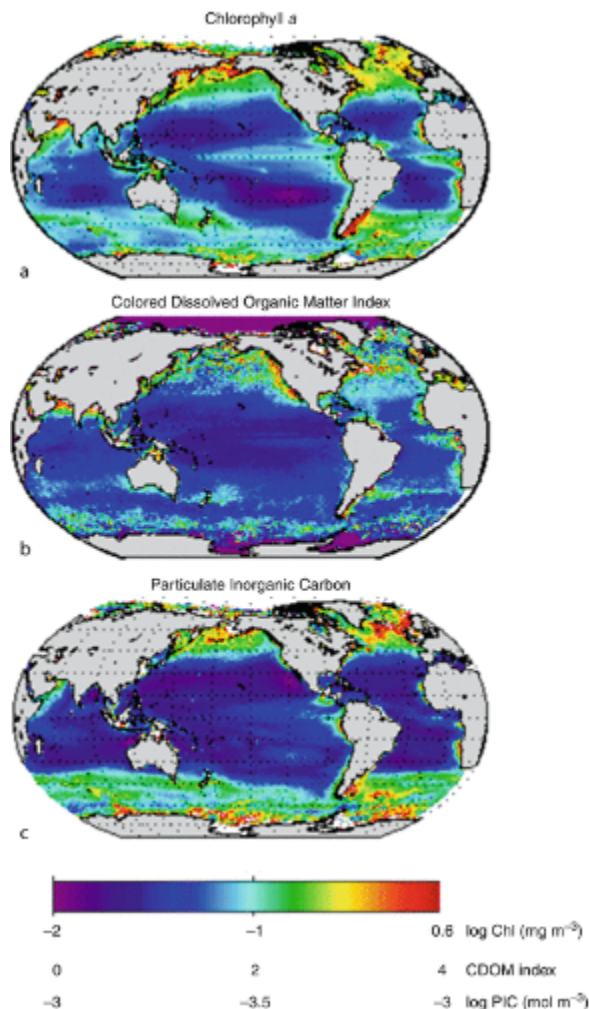
Remote Sensing of Ocean Color. Figure 8 Global climatologies or long-term averages of products derived from the Ocean Color SeaWiFS sensor from 1998-2011. (a) Chlorophyll a (mg m^{-3}); (b) colored dissolved organic matter (CDOM) index; (c) particulate inorganic carbon (PIC) (mol m^{-3})

The relationships between climatological forcing and biological carbon storage in the ocean are complex and not readily incorporated in models. Ocean color imagery can provide assessments of potential changes to ocean processes including primary productivity, surface heating, sediment plumes, altered food webs, harmful algal blooms, changing acidity, and alterations of benthic habitats in response to shifts in winds and upwelling, clouds and radiative forcing, and storm intensity and frequency. Recent observed changes in chlorophyll, primary production, and the size of the oligotrophic gyres from ocean color satellites are compelling evidence of significant changes in the global ocean. A recent study demonstrates that a time series of at least 40 years in length is needed to unequivocally distinguish a global warming trend from natural variability [6] and sustained long-term observations of ocean color are in jeopardy [40].

In addition to sustained imagery, there is a need for integrating ocean color imagery from different platforms to monitor the oceans and aquatic habitats at a variety of desired spectral, spatial, and temporal resolutions. Integration of satellite sensors with suborbital platforms will allow for better assessment of vulnerable marine and aquatic habitats, as well as responses to hazards such as harmful algal blooms, oil spills, and storms that cause coastal flooding and erosion. Active sensors, such as Light Detection and Ranging (LIDAR) , will allow us to probe into the depths of the oceans. Moreover, integrating surface ocean color measurements with three-dimensional measurements and models of the ocean will be increasingly important in discerning a changing ocean [49].

Finally, the approaches or algorithms for conducting ocean color remote sensing will be augmented as more spectral channels become routinely available and as ocean properties change. Purely statistical or empirical models are only accurate when conditions are similar to past conditions. When considering a changing ocean, the cause of the color

change must be carefully assessed to separate the spectral variability due to phytoplankton from other sources of variability, such as sediments, CDOM, and even atmospheric aerosols. Considerable growth is also expected in approaches and technology for remote sensing of coastal habitats and assessing acute and chronic hazards. Comprehensive and consistent field observations from ships to autonomous vehicles and floats are required to assess the accuracy of satellite-derived products, build improved algorithms, and provide better linkages between surface measurements made from space and the processes within the water column [49]. Future effort will also be directed at assimilation of ocean color imagery into global circulation and climate models. As outlined above, remote sensing of ocean color is a complex discipline requiring radiometrically accurate and calibrated sensors, advanced techniques for atmospheric correction of aerosols and dust, and approaches that can deduce the source of variability in the color signal measured by a sensor. With the many important applications of ocean color remote sensing, from climate forecasting to environmental monitoring, a consistent and coordinated international investment in education, research, and technology is required to maintain and advance this dynamic field.

Bibliography

Primary Literature

- 1. Carr ME et al (2006) A comparison of global estimates of marine primary production from ocean color. Deep Sea Res Part II: Top Stud Oceanogr 53:741-770
- 2. Field CB, Behrenfeld MJ, Randerson JT, Falkowski P (1998) Primary production of the biosphere: integrating terrestrial and oceanic components. Science 281:237-240
- 3. Smith RC, Baker KS (1978) Optical classification of natural waters. Limnol Oceanogr 23:260-267
- 4. Martinez E, Antoine D, D'Ortenzio F, Gentili B (2009) Climate-driven basin-scale decadal oscillations of oceanic phytoplankton. Science 326:1253-1256
- 5. Siegel DA, Franz BA (2010) Century of phytoplankton change. Nature 466:569-570
- 6. Henson SA et al (2010) Detection of anthropogenic climate change in satellite records of ocean chlorophyll and productivity. Biogeosciences 7:621-640
- 7. IOCCG (2008) Why ocean colour? the societal benefits of ocean-colour technology. In: Platt T, Hoepffner N, Stuart V, Brown C (eds) Reports of the International Ocean-Colour Coordinating Group, Dartmouth, Canada
- 8. Morel A (1988) Optical modeling of the upper ocean in relation to its biogenous matter content (case I waters). J Geophys Res 93:10749-10768
- 9. Gordon HR, Morel AY (1983) Remote assessment of ocean color for interpretation of satellite visible imagery: a review. Springer, New York
- 10. O'Reilly JE, Maritorena S, Mitchell BG, Siegel DA (1998) Ocean color chlorophyll algorithms for SeaWiFS. J Geophys Res 103:24937-24953
- 11. McClain CR (2009) A decade of satellite ocean color observations*. Annu Rev Mar Sci 1:19-42
- 12. Kirk JTO (1994) Light and photosynthesis in aquatic ecosystems. Cambridge University Press, Cambridge
- 13. Blough NV, Del Vecchio R (2002) Chromophoric DOM in the coastal environment. In: Hansell DA, Carlson CA (eds) Biogeochemistry of marine dissolved organic matter. Academic, San Diego, pp 509-546
- 14. Twardowski MS, Boss E, Sullivan JM, Donaghay PL (2004) Modeling the spectral shape of absorption by chromophoric dissolved organic matter. Mar Chem 89:69-88
- 15. Ciotti AM, Cullen JJ, Lewis MR (2002) Assessment of the relationships between dominant cell size in natural phytoplankton communities and the spectral shape of the absorption coefficient. Limnol Oceanogr 47:404-417
- 16. Bricaud A, Claustre H, Ras J, Oubelkheir K (2004) Natural variability of phytoplanktonic absorption in oceanic waters: influence of the size structure of algal populations. J Geophys Res 109:C11010
- 17. Stramski D, Boss E, Bogucki D, Voss KJ (2004) The role of seawater constituents in light backscattering in the ocean. Prog Oceanogr 61:27-56
- 18. Mobley CD (1994) Light and water: radiative transfer in natural waters. Academic, San Diego
- 19. Gordon HR et al (2009) Spectra of particulate backscattering in natural waters. Opt Express 17:16192-16208
- 20. Twardowski MS, Lewis M, Barnard A, Zaneveld JRV (2005) In-water instrumentation and platforms for ocean color remote sensing applications. In: Miller R, Del-Castillo C, McKeee D (eds) Remote sensing of coastal aquatic waters. Springer, Dordrecht
- 21. Smith RC, Baker K (1978) The bio-optical state of ocean waters and remote sensing. Limnol Oceanogr

23:247-259

- 22. Morel A, Gentilli B (1993) Diffuse reflectance of oceanic waters. II. Bidirectional aspects. Appl Opt 32:6864-6879
- 23. Lee ZP, Carder KL, Arnone RA (2002) Deriving inherent optical properties from water color: a multiband quasi-analytical algorithm for optically deep water. Appl Opt 41:5755-5772
- 24. Aurin DA (2010) Developing ocean color remote sensing algorithms for retrieving optical properties and biogeochemical parameters in the optically complex waters of Long Island Sound. Ph.D. Thesis. University of Connecticut
- 25. Ryan JP et al (2005) Coastal ocean physics and red tides: an example from Monterey Bay, California. Oceanography 18:246-255
- 26. Mouroulis P, Green RO, Wilson DW (2008) Optical design of a coastal ocean imaging spectrometer. Opt Express 16:9087-9096
- 27. Davis CO et al (2002) Ocean PHILLS hyperspectral imager: design, characterization, and calibration. Opt Express 10(4):210-221
- 28. McClain CR, Cleave ML, Feldman GC, Gregg WW (1998) Science quality SeaWiFS data for global biosphere research. Sea Technol 39:10-16
- 29. Gordon HR (1997) Atmospheric correction of ocean color imagery in the Earth Observing System era. J Geophys Res 102:17081-17106
- 30. Antoine D, Morel A (1999) A multiple scattering algorithm for atmospheric correction of remotely sensed ocean color (MERIS instrument): principle and implementation for atmospheres carrying various aerosols including absorbing ones. Int J Remote Sens 20:1875-1916
- 31. Gao BC, Montes MJ, Ahmad Z, Davis CO (2000) Atmospheric correction algorithm for hyperspectral remote sensing of ocean color from space. Appl Opt 39:887-896
- 32. Wang M, Son SH, Shi W (2009) Evaluation of MODIS SWIR and NIR-SWIR atmospheric correction algorithms using SeaBASS data. Remote Sens Environ 113:635-644
- 33. Yan B et al (2002) Pitfalls in atmospheric correction of ocean color imagery: how should aerosol optical properties be computed? Appl Opt 41:412-423
- 34. Fukushima H, Toratani M (1997) Asian dust aerosol: optical effect on satellite ocean color signal and a scheme of its correction. J Geophys Res 102:17119-17130
- 35. Antoine D, Nobileau D (2006) Recent increase of Saharan dust transport over the Mediterranean Sea, as revealed from ocean color satellite (SeaWiFS) observations. J Geophys Res 111:D12214
- 36. Claustre H et al (2002) Is desert dust making oligotrophic waters greener? Geophys Res lett 29:107-1
- 37. Paytan A et al (2009) Toxicity of atmospheric aerosols on marine phytoplankton. Proc Natl Acad Sci 106:4601
- 38. Garrison VH et al (2003) African and Asian dust: from desert soils to coral reefs. Bioscience 53:469-480
- 39. Monahan EC, O'Muircheartaigh I (1981) Improved statement of the relationship between surface wind speed and oceanic whitecap coverage as required for the interpretation of satellite data. In: Gower JFR (ed) Oceanography from space. Plenum, New York, pp 751-755
- 40. National Research Council Committee on Assessing Requirements for Sustained Ocean Color Research and Operations (2011) Assessing requirements for sustained ocean color research and operations. National Academies Press, Washington DC
- 41. Jerlov NG (1974) Optical aspects of oceanography. Academic, London, pp 77-94
- 42. Morel A, Prieur L (1977) Analysis of variations in ocean color. Limnol Oceanogr 22:709-721
- 43. Mobley CD, Stramski D, Bissett WP, Boss E (2004) Optical modeling of ocean water: is the case 1 - case 2 classification still useful? Oceanography 17:60-67
- 44. Morel A, Bricaud A (1981) Theoretical results concerning light absorption in a discrete medium and application to the specific absorption of phytoplankton. Deep-Sea Res 28:1357-1393
- 45. Siegel DA, Maritorena S, Nelson NB, Behrenfeld MJ (2005) Independence and interdependencies among global ocean color properties: reassessing the bio-optical assumption. J Geophys Res 110:C07011
- 46. Swan CM, Siegel DA, Nelson NB, Carlson CA, Nasir E (2009) Biogeochemical and hydrographic controls on chromophoric dissolved organic matter distribution in the Pacific Ocean. Deep Sea Res Part I: Oceanogr Res Pap 56:2175-2192
- 47. Dierssen HM (2010) Benthic ecology from space: optics and net primary production in seagrass and benthic

algae across the Great Bahama Bank. Mar Ecol Progress Ser 411:1-15

- 48. Zaneveld JRV (1989) An asymptotic closure theory for irradiance in the sea and its inversion to obtain the inherent optical properties. Limnol Oceanogr 34:1442-1452
- 49. Dierssen HM (2010) Perspectives on empirical approaches for ocean color remote sensing of chlorophyll in a changing climate. Proc Natl Acad Sci 107:17073
- 50. Moore TS, Campbell JW, Dowell MD (2009) A class-based approach to characterizing and mapping the uncertainty of the MODIS ocean chlorophyll product. Remote Sens Environ 113:2424-2430
- 51. Schofield O et al (2004) Watercolors in the coastal zone: what can we see? Oceanography 17:25-31
- 52. Falkowski P et al (2000) The global carbon cycle: a test of our knowledge of earth as a system. Science 290:291
- 53. Behrenfeld MJ, Falkowski PG (1997) Consumers guide to phytoplankton primary productivity models. Limnol Oceanogr 42:1479-1491
- 54. Campbell J et al (2002) Comparison of algorithms for estimating ocean primary production from surface chlorophyll, temperature, and irradiance. Glob Biogeochem Cycle 16:1035
- 55. Westberry T, Behrenfeld MJ, Siegel DA, Boss E (2008) Carbon-based primary productivity modeling with vertically resolved photoacclimation. Glob Biogeochem Cycle 22:GB2024
- 56. Mouw CB, Yoder JA (2005) Primary production calculations in the Mid-Atlantic Bight, including effects of phytoplankton community size structure. Limnol oceanogr 50(4):1232-1243
- 57. IOCCG (2006) Remote sensing of inherent optical properties: fundamentals, tests of algorithms, and applications. In: Lee ZP (ed) Reports of the International Ocean-Colour Coordinating Group, Dartmouth
- 58. Siegel DA, Maritorena S, Nelson NB, Hansell DA, Lorenzi-Kayser M (2002) Global distribution and dynamics of colored dissolved and detrital organic materials. J Geophys Res 107:3228
- 59. U.S. National Aeronautics and Space Administration, Goddard Earth Sciences, Data and Information Services Center (2011) Giovanni. http://disc.sci.gsfc.nasa.gov/giovanni/
- 60. Behrenfeld MJ et al (2009) Satellite-detected fluorescence reveals global physiology of ocean phytoplankton. Biogeosciences 6:779-794
- 61. Dierssen HM, Kudela RM, Ryan JP, Zimmerman RC (2006) Red and black tides: quantitative analysis of water-leaving radiance and perceived color for phytoplankton, colored dissolved organic matter, and suspended sediments. Limnol oceanogr 51:2646-2659
- 62. Brewin RJW et al (2011) An intercomparison of bio-optical techniques for detecting dominant phytoplankton size class from satellite remote sensing. Remote Sens Environ 115:325-339
- 63. Balch WM, Kilpatrick KA, Trees CC (1996) The 1991 coccolithophore bloom in the central North Atlantic. 1. Optical properties and factors affecting their distribution. Limnol Oceanogr 41:1669-1683
- 64. Tomlinson MC, Wynne TT, Stumpf RP (2009) An evaluation of remote sensing techniques for enhanced detection of the toxic dinoflagellate, Karenia brevis. Remote Sens Environ 113:598-609
- 65. Simis SGH, Peters SWM, Gons HJ (2005) Remote sensing of the cyanobacterial pigment phycocyanin in turbid inland water. Limnol Oceanogr 50:237-245
- 66. Chavez FP, Ryan J, Lluch-Cota SE, Niquen CM (2003) From anchovies to sardines and back: multidecadal change in the Pacific Ocean. Science 299:217-221
- 67. Platt T, Csar Fuentes-Yaco KTF (2003) Marine ecology: spring algal bloom and larval fish survival. Nature 423:398-399
- 68. Fuentes-Yaco C, Koeller PA, Sathyendranath S, Platt T (2007) Shrimp (Pandalus borealis) growth and timing of the spring phytoplankton bloom on the Newfoundland-Labrador Shelf. Fish Oceanogr 16:116-129
- 69. Seibel BA, Dierssen HM (2003) Cascading trophic impacts of reduced biomass in the Ross Sea, Antarctica: just the tip of the iceberg? Biol Bull 205:93-97
- 70. Rosa R, Dierssen HM, Gonzalez L, Seibel BA (2008) Large-scale diversity patterns of cephalopods in the Atlantic open ocean and deep sea. Ecology 89:3449-3461
- 71. Dekker A et al (2005) Remote sensing of seagrass ecosystems: use of spaceborne and airborne sensors. In: Larkum AWD, Orth RJ, Duarte CM (eds) Seagrasses: biology, ecology, and conservation. Springer, Dordrecht, pp 347-359
- 72. Cavanaugh KC, Siegel DA, Kinlan BP, Reed DC (2010) Scaling giant kelp field measurements to regional scales using satellite observations. Mar Ecol Prog Ser 403:13-27

- 73. Phinn S, Roelfsema C, Dekker A, Brando V, Anstee J (2008) Mapping seagrass species, cover and biomass in shallow waters: an assessment of satellite multi-spectral and airborne hyper-spectral imaging systems in Moreton Bay (Australia). Remote sens Environ 112:3413-3425
- 74. Lesser MP, Mobley CD (2007) Bathymetry, water optical properties, and benthic classification of coral reefs using hyperspectral remote sensing imagery. Coral Reefs 26:819-829
- 75. Dierssen HM, Zimmerman RC, Drake LA, Burdige DJ (2009) Potential export of unattached benthic macroalgae to the deep sea through wind-driven Langmuir circulation. Geophys Res Lett 36:L04602
- 76. Burdige DJ, Hu X, Zimmerman RC (2010) The widespread occurrence of coupled carbonate dissolution/reprecipitation in surface sediments on the Bahamas Bank. Am J Sci 310(6):492-521. doi:10.2475/06.2010.03
- 77. Goes JI, Thoppil PG, Gomes HR, Fasullo JT (2005) Warming of the Eurasian landmass is making the Arabian Sea more productive. Science 308:545-547
- 78. Beman JM, Arrigo KR, Matson PA (2005) Agricultural runoff fuels large phytoplankton blooms in vulnerable areas of the ocean. Nature 434:211-214
- 79. Dwivedi RM, Solanki HU, Nayak SR, Gulati D, Somvanshi VS (2005) Exploration of fishery resources through integration of ocean colour with sea surface temperature: Indian experience. IJMS 34:430-440
- 80. Chavez FP, Strutton PG, McPhaden MJ (1998) Biological-physical coupling in the Central Equatorial Pacific during the onset of the 1997-98 El Nino. Geophys Res Lett 25:3543-3546
- 81. Lewis MR, Platt TC (1987) Remote observation of ocean colour for prediction of upper ocean heating rates. Adv Space Res 7:127-130
- 82. Hill VJ (2008) Impacts of chromophoric dissolved organic material on surface ocean heating in the Chukchi Sea. J Geophys Res 113:C07024
- 83. Gnanadesikan A, Anderson WG (2009) Ocean water clarity and the ocean general circulation in a coupled climate model. J Phys Oceanogr 39:314-332
- 84. Gnanadesikan A, Emanuel K, Vecchi GA, Anderson WG, Hallberg R (2010) How ocean color can steer Pacific tropical cyclones. Geophys Res Lett 37:L18802
- 85. Miller WL, Moran MA (1997) Interaction of photochemical and microbial processes in the degradation of refractory dissolved organic matter from a coastal marine environment. Limnol Oceanogr 42:1317-1324
- 86. Ackleson SG, Balch WM, Holligan PM (1994) Response of water-leaving radiance to particulate calcite and chlorophyll a concentrations: a model for Gulf of Maine coccolithophore blooms. J Geophys Res 99:7483-7499
- 87. Gordon HR et al (2001) Retrieval of coccolithophore calcite concentration from SeaWiFS imagery. Geophys Res Lett 28:1587-1590
- 88. Balch W, Drapeau D, Bowler B, Booth E (2007) Prediction of pelagic calcification rates using satellite measurements. Deep Sea Res Part II: Top Stud Oceanogr 54:478-495
- 89. Balch WM, Fabry VJ (2008) Ocean acidification: documenting its impact on calcifying phytoplankton at basin scales. Mar Ecol Prog Ser 373:239-247
- 90. Ryther JH (1969) Photosynthesis and fish production in the sea. Science 166:72-76
- 91. Wilson RW et al (2009) Contribution of fish to the marine inorganic carbon cycle. Science 323:359-362
- 92. Platt T, Sathyendranath S, Fuentes-Yaco C (2007) Biological oceanography and fisheries management: perspective after 10 years. ICES J Marine Sci 64:863
- 93. Platt T, Sathyendranath S (2008) Ecological indicators for the pelagic zone of the ocean from remote sensing. Remote Sens Environ 112:3426-3436
- 94. Stumpf RP et al (2003) Monitoring Karenia brevis blooms in the Gulf of Mexico using satellite ocean color imagery and other data. Harmful Algae 2:147-160
- 95. Hu C et al (2003) MODIS detects oil spills in Lake Maracaibo, Venezuela. Eos AGU Trans 84:313-319
- 96. Fingas M, Brown C (2000) A review of the status of advanced technologies for the detection of oil in and with ice. Spill Sci Technol Bull 6:295-302
- 97. Boland RC, Donohue MJ (2003) Marine debris accumulation in the nearshore marine habitat of the endangered Hawaiian monk seal, Monachus schauinslandi 1999-2001. Mar Pollut Bull 46:1385-1394
- 98. Donohue MJ, Boland RC, Sramek CM, Antonelis GA (2001) Derelict fishing gear in the Northwestern Hawaiian Islands: diving surveys and debris removal in 1999 confirm threat to coral reef ecosystems. Mar Pollut Bull 42:1301-1312

- 99. Randolph K et al (2008) Hyperspectral remote sensing of cyanobacteria in turbid productive water using optically active pigments, chlorophyll a and phycocyanin. Remote Sens Environ 112:4009-4019
- 100. IOCCG (2007) Ocean-colour data merging In: Gregg W (ed) Reports of the International Ocean-Colour Coordinating Group, Dartmouth
- 101. Roy S, Llewellyn C, Egeland ES, Johnsen G (2011) Phytoplankton pigments: updates on characterization, chemotaxonomy and applications in oceanography. Cambridge University Press. Cambridge Environmental Chemistry Series. Cambridge, UK. pp 845. ISBN: 978110700066-7

Books and Reviews

- Campbell J, Antoine D, Armstrong R, Arrigo K, Balch W, Barber R, Behrenfeld M, Bidigare R, Bishop J, Carr ME et al (2002) Comparison of algorithms for estimating ocean primary production from surface chlorophyll, temperature, and irradiance. Glob Biogeochem Cycle 16:1035
- Carr ME, Friedrichs MAM, Schmeltz M, Noguchi Aita M, Antoine D, Arrigo KR, Asanuma I, Aumont O, Barber R, Behrenfeld M et al (2006) A comparison of global estimates of marine primary production from ocean color. Deep Sea ResPart II: Top Stud Oceanogr 53:741-770
- GlobCOLOUR: An EO based service supporting global ocean carbon cycle research. European Space Agency. http://www.globcolour.info/
- IOCCG. Reports of the International Ocean-Colour Coordinating Group No. 1-10. Dartmouth. http://www.ioccg.org/reports_ioccg.html
- Jerlov NG, Nielsen ES (eds) (1974) Optical aspects of oceanography. Academic, London
- Miller R, Del-Castillo C, McKee BA (eds) (2005) Remote sensing of coastal aquatic waters. Springer, Dordrecht
- Morel A (1991) Optics of marine particles and marine optics. In: Demers S (ed) Particle analysis in oceanography. Springer, Berlin, pp 141-188
- Morel A, Bricaud A (1986) Inherent optical properties of algal cells including picoplankton: theoretical and experimental results. Can Bull Fish Aquat Sci 214:521-559
- National Aeronautics and Space Administration (NASA) Ocean optics protocols for satellite ocean color sensor validation, vol I-VI. http://oceancolor.gsfc.nasa.gov/DOCS/
- National Aeronautics and Space Administration (NASA) Ocean color web. http://oceancolor.gsfc.nasa.gov/
- Platt T, Nayak S (eds) (2005). Special issue on: ocean colour remote sensing. Indian J Marine Sci 34(4):341-355
- Siegel D (2004) Views of ocean processes from the sea-viewing wide field- of-view sensor mission: introduction to the first special issue. Deep Sea Res Part II Top Stud Oceanogr 51(1-3):1-3. http://dx.doi.org/10.1016/j.dsr2.2003.12.001
- The Oceanography Society (2004) Special issue: coastal ocean optics and dynamics. Oceanography 17(2):1-95
- Thomas A, Siegel D, Marra J (2004) Views of ocean processes from the sea-viewing wide field- of-view sensor (SeaWiFS) mission: introduction to the second special issue. Deep Sea Res Part II Top Stud Oceanogr 51(10-11):911-912. http://dx.doi.org/10.1016/j.dsr2.2004.06.003

Remote Sensing of Ocean Color

Dr. Heidi M. Dierssen   Department of Marine Sciences, University of Connecticut, Groton, USA

Kaylan Randolph   Department of Marine Sciences, University of Connecticut, Groton, USA